Displacement-Type Ferroelectricity with Off-Center Magnetic Ions in Perovskite $Sr_{1-x}Ba_xMnO_3$

H. Sakai,[1] J. Fujioka,[2] T. Fukuda,[3,4] D. Okuyama,[1] D. Hashizume,[5] F. Kagawa,[6] H. Nakao,[7] Y. Murakami,[7] T. Arima,[8] A. Q. R. Baron,[4,9] Y. Taguchi,[1] and Y. Tokura[1,2,6]

[1]*Cross-Correlated Materials Research Group (CMRG) and Correlated Electron Research Group (CERG), Advanced Science Institute, RIKEN, Wako 351-0198, Japan*
[2]*Multiferroics Project, Japan Science and Technology Agency, Tokyo 113-8656, Japan*
[3]*Synchrotron Radiation Research Unit, SPring-8/JAEA, Hyogo 679-5148, Japan*
[4]*Materials Dynamics Laboratory, RIKEN SPring-8 Center, Hyogo 679-5148, Japan*
[5]*Advanced Technology Support Division, RIKEN, Wako 351-0198, Japan*
[6]*Department of Applied Physics, University of Tokyo, Tokyo 113-8656, Japan*
[7]*Condensed Matter Research Center and Photon Factory, Institute of Materials Structure Science, KEK, Tsukuba 305-0801, Japan*
[8]*Institute of Multidisciplinary Research for Advanced Materials, Tohoku University, Sendai 980-8577, Japan*
[9]*Research and Utilization Division, SPring-8/JASRI, Hyogo 679-5198 Japan*

(Received 1 June 2011; published 19 September 2011)

We report a ferroelectric transition driven by the off-centering of magnetic Mn^{4+} ions in antiferromagnetic Mott insulators $Sr_{1-x}Ba_xMnO_3$ with a perovskite structure. As x increases, the perovskite lattice shows the typical soft-mode dynamics, as revealed by the momentum-resolved inelastic x-ray scattering and far-infrared spectroscopy, and the ferroelectricity shows up for $x \geq 0.45$. The observed polarization is comparable to that for a prototypical ferroelectric $BaTiO_3$. We further demonstrate that the magnetic order suppresses the ferroelectric lattice dilation by ~70% and increases the soft-phonon energy by ~50%, indicating the largest magnetoelectric effects yet attained.

DOI: 10.1103/PhysRevLett.107.137601 PACS numbers: 77.80.−e, 63.20.D−, 75.47.Lx

Since the discovery of ferroelectricity in perovskite $BaTiO_3$ around 1950, a variety of ferroelectric oxides have been extensively studied in the light of electronic device engineering [1] as well as academic interest [2]. More recently, to expand the materials function, multiferroics (magnetic ferroelectrics) have been attracting much attention as well, with the anticipation of realizing large magnetoelectric effects [3,4]. Most of the perovskite ferroelectrics ABO_3 so far identified, however, consist of a nonmagnetic B (transition metal) site with no d-orbital electrons [5]. This empirical rule, so-called "d^0-ness," can be interpreted in terms of the stabilization of the ferroelectric distortion by forming a covalent bond between empty d orbitals of transition metal and filled $2p$ orbitals of oxygen [6]. In contrast, magnetism appears only when the transition metal d orbitals are partially occupied. Such incompatibility between ferroelectricity and magnetism has significantly restricted the variety of multiferroic materials [7,8].

To circumvent this rule, some unconventional mechanisms of ferroelectricity have been exploited. One example is the spin-driven ferroelectrics [3,4], where the polarization is induced as a by-product of spin ordering, as exemplified by perovskite $TbMnO_3$ [9]. While the cross coupling between magnetism and polarization is excellent in this class of multiferroics, the spontaneous electric polarization P_s is typically 2 or 3 orders of magnitude smaller than that for conventional ferroelectrics, and the ferroelectric transition temperature is mostly far below room temperature. As another promising candidate, Bi- or Pb-based ferroelectrics with magnetic B-site ions, such as $BiFeO_3$ and $BiMnO_3$, have attracted significant attention [10,11]. In these materials, the ferroelectricity stems from the $6s$ lone pair in the Bi ion, indicating that the ferroelectric and magnetic orders are associated with different ions [12]. Consequently, the coupling between them is weak [13].

Recently, several first-principles calculations have pointed out the possible ferroelectric ground state with large P_s (tens of $\mu C/cm^2$) for $AMnO_3$ (A = Ca, Sr, and Ba), accompanied by the Mn^{4+} ion displacement in which the strong Mn-O bond covalency may persist [14–16]. The ferroelectric instability was predicted to increase with increasing the lattice constant by changing the A-site ion from Ca through Sr to Ba. In reality, cubic $SrMnO_3$ is a typical Mott insulator with G-type (staggered in all three directions) antiferromagnetism and paraelectric down to the lowest temperature [17]. Further expansion of the lattice by partially substituting Sr with Ba is anticipated to cause the ferroelectric transition, but at up to 20% Ba substitution no ferroelectric transition was observed [17]. For a larger lattice constant, the hexagonal polymorph becomes so stable that the cubic perovskite structure cannot be synthesized by the conventional solid-state reaction [18]. To overcome this problem, we have developed a two-step crystal growth technique, consisting of a floating-zone

method and high-pressure oxygen annealing [19]. This enabled the synthesis of single crystals with the perovskite structure up to 50% Ba substitution. In this Letter, we describe a ferroelectric transition in the highly Ba-doped crystals, originating from the off-centering of the magnetic B-site ions. In addition to large P_S ($\sim 4.5\ \mu C/cm^2$ for heavily twinned specimens), the ferroelectric distortion as well as the relevant soft-phonon mode were found to show a huge variation upon the magnetic order, indicating the strongest magnetoelectric coupling hitherto known.

Single crystals of $Sr_{1-x}Ba_xMnO_3$ ($0 \le x \le 0.5$) were synthesized as follows: We first grew oxygen-deficient single crystals with an orthorhombic or cubic perovskite structure with a floating-zone method in an argon atmosphere at the growth speed of 2–10 mm/h. Pieces of the crystals were then annealed with an oxidizing agent ($NaClO_3$) by using a cubic anvil-type high-pressure apparatus (~ 6.5 GPa, $\sim$480 °C). Dielectric permittivity up to 1 MHz was measured by an LCR (inductance-capacitance-resistance) meter, while an impedance analyzer was utilized for 1 MHz–1.3 GHz. Electric polarization was measured by a commercial ferroelectric tester. Optical reflectivity was measured by a Fourier-transform infrared spectrometer (0.005–0.5 eV), a grating spectrometer (0.5–5 eV), and synchrotron radiation at UV-SOR, Japan (5–40 eV). Optical conductivity and dielectric spectra were calculated by Kramers-Kronig analysis. Inelastic x-ray scattering was performed at beam line 35XU [20], SPring-8, Japan. Single-crystal x-ray diffraction was performed at beam line 8A, Photon Factory, KEK, Japan. Powder x-ray measurements were performed by using an in-house diffractometer. (For further details, see Supplemental Materials [21].)

Figure 1 shows an overview of the lattice, magnetic, and dielectric properties for $Sr_{1-x}Ba_xMnO_3$ ($0 \le x \le 0.5$). With increasing x from 0 to 0.4, the lattice constant a at 300 K monotonically increases from 3.807 to 3.856 Å with keeping the cubic symmetry [Fig. 1(b)]. Around $x = 0.45$, however, the crystal structure changes from cubic to tetragonal, indicating ferroelectric distortion with an elongation of the c axis. The ferroelectric transition temperatures T_C [Fig. 1(a)] were determined as the temperatures where this tetragonal distortion vanishes [Fig. 3(c)]. Judging from the temperature profiles of magnetization [21], the antiferromagnetic-transition temperature T_N gradually decreases from 230 ($x = 0$) to 185 K ($x = 0.5$) [22]. For $x \ge 0.45$, a novel multiferroic phase thus appears below $T_N(<T_C)$, associated with the antiferromagnetic ordering of off-center Mn^{4+} ions [Fig. 1(a)].

The ferroelectric transition in $Sr_{1-x}Ba_xMnO_3$ is governed by a soft phonon, reflecting the displacement-type ferroelectricity. Figure 2(a) shows the spectra of the imaginary part of dielectric constant $\varepsilon_2(\omega)$ for the $x = 0$–0.3 crystals at 300 K. In all of these compounds, three intense transverse optical phonons (TO1–3) were observed,

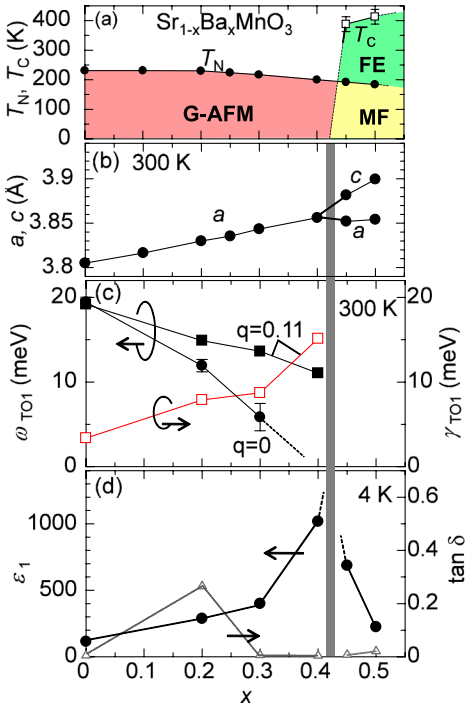

FIG. 1 (color online). (a) Phase diagram for $Sr_{1-x}Ba_xMnO_3$ as a function of x. G-AFM, FE, and MF denote G-type antiferromagnetic, ferroelectric, and multiferroic phases, respectively. T_N was deduced from the temperature profiles of magnetization [21]. (b) Variation in the lattice constant at 300 K. (c) Variation in the soft-mode energy (ω_{TO1}) at 300 K at the wave vector of $q = 0$ and 0.11, determined from the optical spectra and inelastic x-ray scattering, respectively. The linewidth (γ_{TO1}) at $q = 0.11$ is also plotted. (d) Variation in dielectric constant ε_1 (left axis) and loss tanδ (right axis) at 4 K. For $x = 0.2$, 0.3, and 0.4 with a relatively large leakage current (larger tanδ), the values at 1 GHz are plotted to minimize the carrier hopping contribution [21], while those at 1 MHz are plotted for other well-insulating compounds.

corresponding to the triply degenerate T_{1u} modes in the cubic $Pm\bar{3}m$ space group. Only the TO1 mode shows significant softening with increasing x. As shown in Fig. 1(c) ($q = 0$), the energy of the TO1 mode steeply decreases toward zero as x approaches the ferroelectric phase. In accordance with this behavior, the real part of dielectric permittivity ε_1 at 4 K rapidly increases as the ferroelectric phase is approached, exceeding 1000 for $x = 0.4$ [Fig. 1(d)]. In the ferroelectric phase, on the other hand, it is largely reduced to $\sim$200 for $x = 0.5$.

The soft mode was further investigated by measuring phonon dispersion along the [110] direction [Figs. 2(b)–2(e)], by inelastic x-ray scattering. The measurements were performed around the 005 Bragg reflection to detect the phonons with polarization vector ξ parallel to [001], using single crystals with a typical dimension of $\sim 1 \times 1 \times 1\ mm^3$ [21]. The dispersion of the TO1 mode markedly varies with x, whereas those of the acoustic mode (TA) and

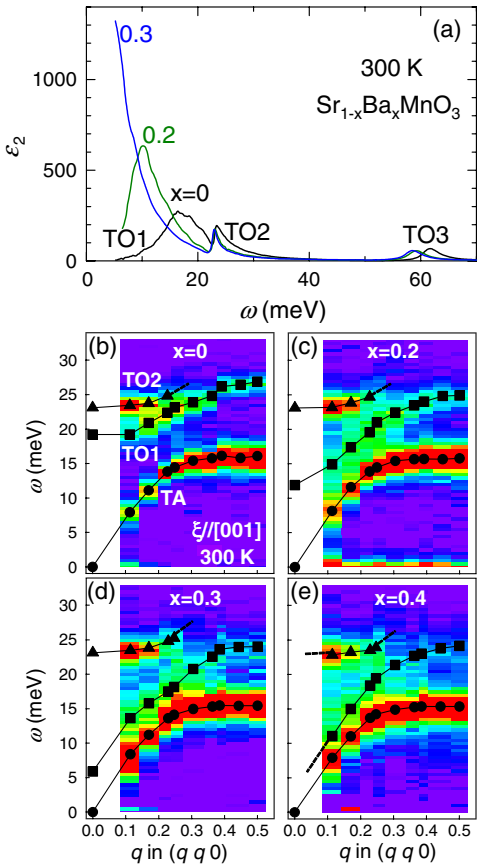

FIG. 2 (color online). (a) Imaginary part of dielectric permittivity ε_2 as a function of photon energy ω for $x = 0$–0.3, deduced from the reflectivity measurements ($q = 0$). Plots of the inelastic-x-ray-scattering intensity at 300 K in the energy-wave-vector (ω-q) plane in the [110] (Γ-M) direction for (b) $x = 0$, (c) 0.2, (d) 0.3, and (e) 0.4, measured around 005 reflection. The closed symbols denote the phonon frequency ω_q, obtained by the fitting based on the damped harmonic oscillators [21]. The points at $q = 0$ were determined from the optical spectra.

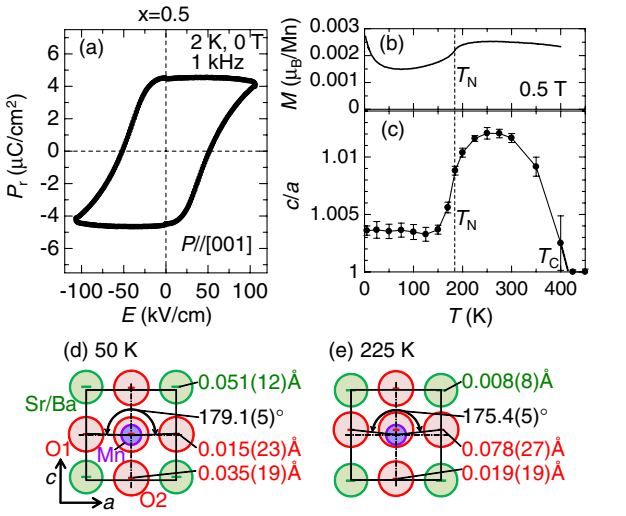

FIG. 3 (color online). (a) Remnant P-E hysteresis curve (2 K, 1 kHz, 0 T) along [001] in the pseudocubic setting for $x = 0.5$, where the specimen was heavily twinned. The nonswitching components arising from leakage current and field-induced polarization are subtracted [21]. Temperature profiles of (b) magnetization M at 0.5 T and (c) tetragonality c/a for $x = 0.5$. The values of c/a were estimated from the split of the 002/200 peaks in powder x-ray diffraction. Schematic diagrams for the crystal structure at (d) 50 and (e) 225 K, deduced from the single-crystal x-ray diffraction. Each atomic displacement is shown on the basis of the Mn-centered unit cell.

TO2 do not change notably. With increasing x, the TO1 branch shows significant softening and damping near the Γ point, resulting in the overdamped behavior (i.e., the phonon energy is smaller than its linewidth) in the small-q region for $x = 0.4$ [Fig. 1(c)]. Magnetic fluctuation may have a substantial contribution to such heavy damping, since the linewidth of the TO1 mode steeply decreases below T_N. (see Fig. 4).

P_s along the c axis has been clearly observed in the P-E hysteresis curve for $x = 0.5$, as shown in Fig. 3(a). The measured value at 2 K is $\sim$4.5 μC/cm^2 in a specimen with heavily twinned tetragonal domains, suggesting the intrinsic P_s value of 13.5 μC/cm^2($= 4.5 \times 3$) for a single domain. This value may be further enhanced, perhaps up to $\sim$25 μC/cm^2 as a maximum above T_N, as discussed later. Thus, the values of P_s and T_C for $x = 0.5$ are comparable with those for $BaTiO_3$ ($P_s = 26$ μC/cm^2 and $T_C = 406$ K). Since there are no lone pairs in Sr^{2+}/Ba^{2+} ions, the observed ferroelectricity is attributed to the displacement of the magnetic Mn^{4+} ions with d^3 configuration, violating the d^0-ness requirement.

The long-range ordering of Mn^{4+} spins has strikingly large effects on P_s and lattice distortion. For ferroelectric $x = 0.5$, the temperature profile of magnetization shows a clear anomaly at 185 K, corresponding to T_N [Fig. 3(b)]. The detailed crystal structures for this compound at 50 K (below T_N) and at 225 K (above T_N) were deduced from the single-crystal diffraction using the synchrotron x-ray method, as shown in Figs. 3(d) and 3(e), respectively. Considering the ferroelectric ground state, we have determined the space group at 50 K as noncentrosymmetric $P4mm$ and assumed the same space group at 225 K. The obtained reliability factors are $R = 2.76\%$ and 1.84% at 50 and 225 K, respectively [23]. The shift of Mn^{4+} ion from the center of the surrounding oxygens is suppressed below T_N. The Mn-O-Mn bond deviates significantly from 180° above T_N [$\sim$ 175.4(5)°] but becomes close to 180° below T_N [$\sim$ 179.1(5)°]. This is highlighted by the temperature profile of c/a [Fig. 3(c)]. The c/a value, which reaches 1.012 around room temperature, begins to decrease with decreasing temperature around 225 K ($> T_N$), probably due to the antiferromagnetic fluctuation, and then steeply drops at T_N. Below 150 K, the c/a value is almost constant ($\sim$ 1.0035), at approximately 30% of the maximum deviation from the cubic value ($c/a = 1$).

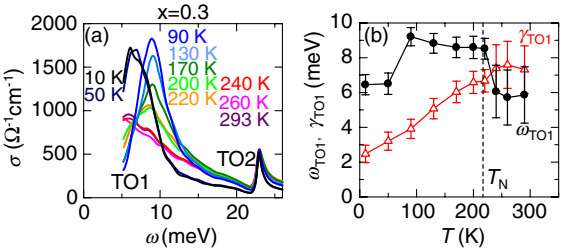

FIG. 4 (color online). (a) Optical conductivity σ as a function of photon energy ω at various temperatures for $x = 0.3$. (b) Temperature dependence of soft-mode (TO1) energy ω_{TO1} and linewidth γ_{TO1} for $x = 0.3$, obtained by fitting the reflectivity spectra to the Lorentz oscillator model [21].

The mechanism of such strong suppression of tetragonal distortion (and presumably of ferroelectricity) upon the antiferromagnetic order can be explained in terms of the superexchange interaction between Mn^{4+} spins. Since the 180° Mn-O-Mn bond is energetically favored for the antiferromagnetic coupling [24,25], Mn and O ions shift so as to make the bond angle close to 180° when the antiferromagnetic order (or fluctuation) occurs. As a simple estimation of the corresponding change in P_s, we here assume $(c/a - 1) \propto P_s^2$ by neglecting the direct contribution from magnetostriction effects. The P_s value above T_{N} is then estimated from the temperature variation of c/a to be about 1.9 times as large as that below T_{N}: $\sim 25\ \mu\mathrm{C/cm^2}$ as a maximum. The antiferromagnetic ordering thus can produce huge variation in P_s of the order of $\mu\mathrm{C/cm^2}$.

Strong coupling with antiferromagnetism is also prominent in the soft-mode behavior in the paraelectric systems. Figure 4(a) shows optical conductivity spectra from 293 to 10 K for the $x = 0.3$ crystal. The TO1 appears to be located around 6 meV above T_{N}. It shows a dramatic hardening at T_{N} accompanied by the peak narrowing, whereas the higher-lying TO2 mode shows almost no temperature dependence. Figure 4(b) summarizes the temperature dependence of the energy and linewidth of the TO1 mode. Above T_{N}, although the TO1 mode is too low in energy (~ 6 meV) to determine the temperature variation precisely, it might slightly soften with decreasing temperature. Below T_{N}, in contrast, the mode energy increases and reaches 9 meV around 100 K. As the temperature is decreased further, the TO1 mode softens again. While the current leakage of the crystal hindered the direct dielectric measurement around T_{N}, the Lyddane-Sachs-Teller relation allows us to estimate the drop in dielectric constant at T_{N} to be $\sim 60\%$ from the observed energy shift (more than 3 meV), suggesting again significant magnetoelectric coupling.

The nonmonotonic temperature dependence of the soft-mode energy can be explained by considering the spin-phonon coupling [26,27]: $\omega_{\mathrm{TO1}}^2 = \omega_0^2 + \lambda\langle S_i \cdot S_j \rangle$, where ω_0 is a phonon frequency without magnetism, λ is a coupling constant, and $\langle S_i \cdot S_j \rangle$ is the nearest-neighbor spin correlation function. The temperature dependence of ω_0 should be expressed as $\omega_0^2 \propto (T - T_{\mathrm{C}}')$, assuming the conventional soft-mode behavior above T_{N}. T_{C}' is the fictitious ferroelectric transition temperature without magnetism. The evolution of the second term due to the antiferromagnetic ordering should result in steep hardening below T_{N}. For $T_{\mathrm{C}}' \ll T_{\mathrm{N}}$, the resoftening toward 0 K observed for $x = 0.3$ can be reproduced, since the $\langle S_i \cdot S_j \rangle$ value almost saturates well below T_{N}.

The authors are grateful to Y. Tokunaga, S. Ishiwata, and R. Kumai for fruitful discussions. The measurements in SPring-8 were performed under Proposals No. 2010A1552 and No. 2010B1579. The measurements in KEK were performed under Proposal No. 2009S2-008. This study was partly supported by Special Postdoctoral Program in RIKEN, KAKENHI 22740244, and Funding Program for World-Leading Innovative R&D on Science and Technology on "Quantum Science on Strong Correlation."

[1] J. F. Scott, Science **315**, 954 (2007).
[2] M. Dawber, K. M. Rabe, and J. F. Scott, Rev. Mod. Phys. **77**, 1083 (2005).
[3] S. W. Cheong and M. Mostovoy, Nature Mater. **6**, 13 (2007).
[4] Y. Tokura and S. Seki, Adv. Mater. **22**, 1554 (2010).
[5] B. T. Matthias, Phys. Rev. **75**, 1771 (1949).
[6] R. E. Cohen, Nature (London) **358**, 136 (1992).
[7] N. A. Hill, J. Phys. Chem. B **104**, 6694 (2000).
[8] D. I. Khomskii, J. Magn. Magn. Mater. **306**, 1 (2006).
[9] T. Kimura, T. Goto, H. Shintani, K. Ishizaka, T. Arima, and Y. Tokura, Nature (London) **426**, 55 (2003).
[10] For a review, see G. Catalan and J. F. Scott, Adv. Mater. **21**, 2463 (2009).
[11] J. Wang, J. B. Neaton, H. Zheng, V. Nagarajan, S. B. Ogale, B. Liu, D. Viehland, V. Vaithyanathan, D. G. Schlom, U. V. Waghmare, N. A. Spaldin, K. M. Rabe, M. Wuttig, and R. Ramesh, Science **299**, 1719 (2003).
[12] R. Seshadri and N. A. Hill, Chem. Mater. **13**, 2892 (2001).
[13] T. Kimura, S. Kawamoto, I. Yamada, M. Azuma, M. Takano, and Y. Tokura, Phys. Rev. B **67**, 180401 (2003).
[14] S. Bhattacharjee, E. Bousquet, and P. Ghosez, Phys. Rev. Lett. **102**, 117602 (2009).
[15] J. M. Rondinelli, A. S. Eidelson, and N. A. Spaldin, Phys. Rev. B **79**, 205119 (2009).
[16] J. H. Lee and K. M. Rabe, Phys. Rev. Lett. **104**, 207204 (2010).
[17] O. Chmaissem, B. Dabrowski, S. Kolesnik, J. Mais, D. E. Brown, R. Kruk, P. Prior, B. Pyles, and J. D. Jorgensen, Phys. Rev. B **64**, 134412 (2001).
[18] Y. Syono, S. Akimoto, and K. Kohn, J. Phys. Soc. Jpn. **26**, 993 (1969).
[19] H. Sakai, S. Ishiwata, D. Okuyama, A. Nakao, H. Nakao, Y. Murakami, Y. Taguchi, and Y. Tokura, Phys. Rev. B **82**, 180409(R) (2010).

[20] A. Q. R. Baron, Y. Tanaka, S. Goto, K. Takeshita, T. Matsushita, and T. Ishikawa, J. Phys. Chem. Solids **61**, 461 (2000).

[21] See Supplemental Material at http://link.aps.org/supplemental/10.1103/PhysRevLett.107.137601 for detailed methods, fitting procedure, and magnetic and dielectric properties.

[22] In the tetragonal phase, the *G*-type antiferromagnetism might be slightly modulated due to the Dzyalonshinsky-Moriya interaction.

[23] We have also analyzed the crystal structure at 225 K by assuming centrosymmetric $P4/mmm$ and obtained reliability factors comparable to those in the noncentrosymmetric case. However, $P4mm$ should be more plausible at 225 K, since the ferroelectric instability is further enhanced in the paramagnetic phase, as indicated by the temperature dependence of soft-phonon energy (Fig. 4).

[24] J. B. Goodenough, Phys. Rev. **100**, 564 (1955).

[25] J. Kanamori, J. Phys. Chem. Solids **10**, 87 (1959).

[26] T. Katsufuji and H. Takagi, Phys. Rev. B **64**, 054415 (2001).

[27] C. J. Fennie and K. M. Rabe, Phys. Rev. Lett. **97**, 267602 (2006).